Colloids and Surfaces A: Physicochem. Eng. Aspects 520 (2017) 779–787

Contents lists available at ScienceDirect

Colloids and Surfaces A: Physicochemical and Engineering Aspects

journal homepage: www.elsevier.com/locate/colsurfa

Hydrophilic and hydrophobic tail effects on vesicle formation in a non-ionic surfactant aqueous solution below the Krafft temperature

Youhei Kawabata*, Kana Ohmoto, Akira Murakami, Yuto Takahashi, Yousuke Yamauchi, Tadashi Kato

Department of Chemistry, Tokyo Metropolitan University, Hachioji, Tokyo 192-0397, Japan

HIGHLIGHTS

- Lamellar domain structures in a non-ionic surfactant C_iE_j aqueous solution below the Krafft temperature are investigated.
- The morphologies of the lamellar structures were summarized into the *i*–*j* diagram.
- Vesicles can be formed at a certain hydrophilicity.
- At the lower hydrophilicity, network and crystal-like structures are formed, and at the higher hydrophilicity, lamellar domains are not grown.

GRAPHICAL ABSTRACT

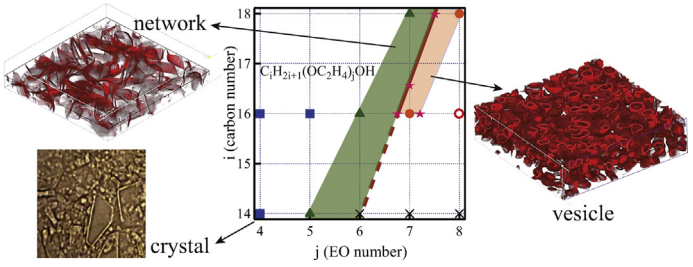

ARTICLE INFO

Article history:
Received 11 November 2016
Received in revised form 24 January 2017
Accepted 30 January 2017
Available online 6 February 2017

Keywords:
Krafft phenomenon
Non-ionic surfactant
HLB
Vesicle

ABSTRACT

In our previous study, we found that multilamellar vesicles are always formed spontaneously in a non-ionic polyoxyethylene-type surfactant $C_{i=16}E_{j=7}$ aqueous solution below the Krafft temperature [9]. It has also been shown that vesicles are not formed when the hydrophilicity of the surfactant molecules decreases. In this study, we investigated the hydrophilic or hydrophobic tail effects on the formation of vesicles through the microscope observation of the C_iE_j/water system. We found that the vesicles are also formed in $C_{18}E_8$/water systems. Furthermore, the morphologies of the lamellar structures and the conditions of vesicle formation were summarized into the *i*–*j* diagram based on the results obtained from the observations of $C_{i=14,16,18}E_j$ systems and the mixture systems $C_{16}E_7/C_{16}E_8$, $C_{16}E_7/C_{18}E_7$, $C_{16}E_7/C_{18}E_8$ and $C_{18}E_7/C_{18}E_8$. We concluded that vesicles can be formed at a certain level of hydrophilicity.

1. Introduction

Surfactant molecules self-assemble to form various structures, such as micelles, lamellae and cubic-type ordered structures, which have always been investigated from the viewpoint of physical or chemical fundamental interests. These self-assembled structures have been applied to industrial and medical fields [1–3].

In a surfactant aqueous solution, crystallization of surfactant bilayers (L_c phase) occurs below the Krafft temperature, which corresponds to the melting temperature of hydrophobic parts of a surfactant [4–6,2]. For the Krafft phenomenon, the lamellar gel phase (L_β), whose lamellar ordering is lower than that of L_c, has been reported [7,8]. In general, the lamellar repeat distance of L_β is larger than that of L_c, and vesicles sometimes can be formed in

* Corresponding author.
E-mail address: youheik@tmu.ac.jp (Y. Kawabata).

http://dx.doi.org/10.1016/j.colsurfa.2017.01.090
0927-7757/

the L_β phase because their bilayer structures are more flexible than those of the L_c phase.

On the other hand, we have found a transition corresponding to the Krafft phenomenon, where the micellar phase transforms the interdigitated lamellar phase (L_β) into a mono long-alkyl non-ionic surfactant/water system [9–13]. In polyoxyethylene-type non-ionic surfactant $C_{16}E_j$ systems ($C_{16}E_j$ is the abbreviation of $C_{16}H_{33}(OC_2H_4)_jOH$), the solutions present a strong turbidity and gel or sol-like features below the Krafft temperature. In the $C_{16}E_6$/water system, lamellar domains consisting of multi-bilayers (L_β phase) are organized randomly (network structures) and in the $C_{16}E_7$/water system, on the other hand, multilamellar films close spontaneously to become spherical vesicles with a hollow that retains excess of water [9,10,12]. This spontaneous vesicle formation occurs in a wide concentration range, and at the lowest concentration limit, disk/vesicle transition is induced by changing concentration or temperature [13]. Furthermore, in mixed systems such as $C_{16}E_6/C_{16}E_7$/water, network structures transform into vesicles at around the $C_{16}E_7$ mixture fraction $\gamma_{C_{16}E_7} = 0.8$. We consider that this large hydrophilicity is one of the factors of vesicle formation induced by Krafft transition [11].

In this study, to clarify the hydrophilic and hydrophobic tail effects on vesicle formation in a C_iE_j/water system, we carried out confocal microscopy (CFM) observations and dynamic light scattering (DLS) experiments. Especially, we focused on the $C_{18}E_j$ system and found that the vesicle formation occurs in $C_{18}E_8$, while the network structure is formed in the $C_{18}E_7$ system. Furthermore, we observed the domain morphology in the $C_{i=14,16}E_j$ systems and the mixture systems $C_{16}E_7/C_{16}E_8$, $C_{16}E_7/C_{18}E_7$, $C_{16}E_7/C_{18}E_8$ and $C_{18}E_7/C_{18}E_8$ through confocal microscopy. The results are summarized in a morphological diagram whose axes represent the carbon number of the alkyl chain and the number of ethylene oxide groups.

2. Experiments

2.1. Sample preparation

Samples were prepared by mixing $C_{18}E_7$ or $C_{18}E_8$ with deuterated water (D_2O) so that the surfactant concentration became 0.01–0.05, 0.1 and 10 wt% for the DLS, microscope and DSC experiments, respectively. For the morphological diagram, we analysed the microscope images related to the total surfactant concentrations of 0.1 and 10 wt%. Note that vesicles in the $C_{16}E_7$ system are formed between 0.02 and 40 wt%, and that in the mixture system ($C_{16}E_6/C_{16}E_7$), vesicle formation depends mainly on the mixing ratio, although there is a slight dependence of temperature on domain morphology (see the supporting information). D_2O was used for comparison with our previous results obtained in the $C_{16}E_j/D_2O$ systems, and purified H_2O was prepared for the DLS experiments. $C_{18}E_7$, $C_{18}E_8$ and the other C_iE_j were purchased from Nikko Chemicals Inc. in crystalline form and used without further purification. Before mixing, the water was bubbled by nitrogen to avoid oxidation of the ethylene oxide group of the surfactants [14]. The mole fraction $\gamma_{C_{18}E_8}$ of $C_{18}E_8$ in total surfactants was 0.2–0.8.

The fluorescent molecule used for confocal microscope observations was lipophilic tracer DiI (Invitrogen Inc., 1,1,-dihexadecyl-3,3,3,3-tetramethy-lindocarbocyanine perchlorate, with excitation and emission wavelengths of 549 and 565 nm, respectively) [12], and was mixed with the surfactants at 0.1 wt%.

2.2. Experimental method

For determining the Krafft temperature T_K, DSC measurements were performed using a DSC 120 (SII Nano Technology Co., Ltd.). The used samples were hermetically sealed with 7 μl Ag pans obtained from SII Nano Technology Co., Ltd. Temperature was increased from 0 to 50 °C at a rate of 1 °C/min. The Krafft temperatures were also visually determined by changing the water bath temperature and inspecting the scattered and the transmitted light. The water bath temperature was controlled at a cooling rate of 0.5 K/min.

For the confocal microscope observations, we used FV-300 (Olympus Inc.). Temperature was controlled by using a hot stage 10002L (Linkam Scientific Instruments Ltd.). The samples were placed between two pieces of glass covers with a 0.2-mm-thick spacer. The covered samples were fixed to copper disks and placed in the sample chamber for the hot stage. The excitation laser for the confocal microscope was He–Ne green laser whose wavelength was 543 nm. We observed the lamellar domain structures at 30–60 min after the temperature was quenched under 3–8 °C from the Krafft temperature of each sample at a rate of 5 °C/min. Note that the domain structures grow with time for about 30 min, and the domain growth is almost saturated after 30 min from temperature quench.

The DLS experiments were performed with a mono mode-fibre compact goniometer system (ALV/LSE-5004) by using a diode-laser pumped Nd–YAG laser (wavelength in vacuum was 532 nm). The scattering angle was set at 50–110 °. The cylindrical cells made of quartz were used with the samples and placed into the cell housing, whose temperature was controlled by a water circulator. All DLS experiments were conducted during 24 h after the temperature was quenched under 6–8 °C from the Krafft temperature of each sample.

Small/wide-angle X-ray scattering (SAXS/WAXS) experiments were performed using a NANO-Viewer (Rigaku Inc.). The scattered X-ray was detected by a pilatus (Dectris Inc.) for SAXS and an imaging plate for WAXS. The q ranges were 0.1–2.5 nm^{-1} for SAXS and 10–35 nm^{-1} for WAXS. The used sample cell for the SAXS/WAXS experiments was made of copper with Kapton windows and the sample thickness was 1 mm. The sample cell was set in a hot stage TS-62 with mk-1000 (Instec Inc.), and the sample temperature was controlled using the hot stage with a precision of ±0.1 °C. The temperature condition was the same as that for the microscope experiment.

3. Results and discussion

3.1. Krafft temperature

Fig. 1a shows the typical DSC curves at various mole fractions $\gamma_{C_{18}E_8}$ of the $C_{18}E_7/C_{18}E_8$ system. The endothermic peaks correspond to that of the melting hydrophobic tails. In order to confirm it, we checked the SAXS and WAXS profiles of the $C_{18}E_8$ system below the temperature of the endothermic peak. As shown in the supporting information, the peaks were confirmed at $q = 0.7$ and 1.4 nm^{-1} of the SAXS profiles and at $q = 15$ nm^{-1} of the WAXS profiles, which correspond to lamellar bilayer planes of hexagonal order. These results are consistent with our previous results [11], so we considered that the endothermic peaks correspond to Krafft transition. For the DSC curve, T_K was estimated by the crossing point of the linear dropping part of the peak and the background average. The determined T_K was confirmed to be consistent with the estimated value by visual inspection of the samples [11]. Fig. 1b shows the $\gamma_{C_{18}E_8}$ dependence of the obtained T_K. The Krafft temperature decreases monotonously with increasing $\gamma_{C_{18}E_8}$. This tendency is consistent with that obtained in the $C_{16}E_j$ systems [11]. The Krafft temperature of each system with other combinations of i and j is summarized in Fig. 2. The colour variation corresponds to the Krafft temperature and the inset in the figure is the ethylene oxide (EO) number dependence of T_K at the carbon umber of 16. It is clear that T_K increases under the lower hydrophilic condition (larger i and less j) and decreases rapidly with increasing EO number.